THE EFFECT OF PHYSIOLOGICAL LOAD CONFIGURATION ON INTERFACE MICROMOTION IN CEMENTLESS FEMORAL STEMS

Mohammed Rafiq Abdul Kadir[1*], Ulrich N. Hansen[2]

[1*]Biomechanics & Tissue Engineering Group (Bio-TEG),
Faculty of Mechanical Engineering,
Universiti Teknologi Malaysia.

[2]Biomechanics Laboratory,
Department of Mechanical Engineering,
Imperial College London.

ABSTRACT

The most commonly reported failure modes of cementless hip stems are loosening and thigh pain; both are attributed to the relative motion at the bone-implant interface due to failure to achieve sufficient primary fixation. Accurate predictions of hip stems' stability are therefore crucial to the pre-clinical analyses of hip arthroplasty. This study uses finite element technique to analyse the effect of muscle forces on the predicted micromotion and therefore stability of cementless femoral components. An in-house experimentally validated micromotion algorithm was used in analyses simulating two of the most common physiological activities– walking and stair-climbing. The results showed that models where muscle loads were included had ten times larger micromotion than those modelled without muscle loads. Ignoring muscle forces in any pre-clinical evaluation of femoral stems are therefore not advisable as it will overestimate the stability of the stem.

Keywords: *Hip arthroplasty, cementless stem, finite element, muscle loadings primary stability, interface micromotion*

1.0   INTRODUCTION

Primary stability is crucial to the short-term and long-term success of cementless femoral prostheses. Unstable implants can cause complications such as thigh pain [1-3] and the eventual loosening of the prosthesis [4-6]. Various design parameters had been studied in order to achieve adequate stability in a hip arthroplasty using a cementless technique [7-9]. However, the effect of including the muscle forces has not received much attention. Due to the complexity of muscle loadings and variations between patients, most experimental studies as well as finite element

---

[*] Corresponding author: E-mail: rafiq@fkm.utm.my

studies did not include muscle forces in their models [10-15] and only a few included either the abductor or the adductor muscles [16,17].

Using finite element (FE) techniques, several investigators reported that muscle forces have an impact on stress distribution in the femur [18-20], whilst others found that including the muscle forces is important for accurate predictions of bone resorption [21]. Various other researchers presented FE studies related to micromotion [22-27], but the effect of muscle loads on the accuracy of micromotion predictions are still remain to be answered.

When analysing the effect of muscle loads, one consideration which is important to micromotion predictions is the type of physical activity. Modelling the changing load configuration during physiological gait cycle, running, and stairclimbing as well as any other physical activities is not practical. Gait is clearly relevant for a study on hip stem's stability as this is the most common physiological activity. Stairclimbing is another important activity due to a high torsional load component which is thought to be particularly critical with respect to interface micromotion [28]. As a consequence, previous works on hip arthroplasty and micromotion had used either gait loading or stairclimbing loads. However, the effects of these loadings on predicted micromotions had not been evaluated.

In this study the effects of muscle loads on interface micromotion were assessed to see whether or not it was important to include muscle loads when predicting the stability of cementless hip stems. Loading configurations from two of the most common physiological activities were used to identify the most relevant and the most critical activity to the stability of cementless hip stems.

2.0   MATERIALS AND METHODS

A 3D model of the hip was constructed from the Visible Human Project (VHP) Computed Tomography (CT) images using AMIRA software (Mercury Computer Systems, Inc.). Segmentation of the 2D slices was carried out manually and complied automatically to generate a 3D triangular surface mesh. The model was then converted to solid tetrahedrals in Marc-Mentat (MSC Software) FE software. A generic 3D CAD model of a stem with straight cylindrical design was also constructed and meshed in solid tetrahedrals. The stem was aligned inside the femur, and the neck of the femur was resected at about 10mm above the upper end of the lesser trochanter to simulate hip replacement. The stem was assigned a linear isotropic material properties resembling titanium alloy (E=110GPA, v=0.3), whilst the properties of the bone were assigned according to the grey level values of the CT dataset. An in-house algorithm was used to correlate the grey-level of the CT images using the apparent density through cubic correlation proposed by Carter and Hayes [29]:

$$E = c\rho^3$$
where E = stiffness of bone (N/m^2)
         c = constant (3,790MPa.cm^9/g^3)
         ρ = density of bone (kg/m^3)

This relationship is based on the assumption that cancellous and cortical bones are simply at different ends of a continuous spectrum. A mesh convergence study was carried out, and the model with 56,526 elements and 12,078 nodes were found to be adequate to produce a converged solutions.

A direct contact method at the interface was used, where a constraint was automatically imposed when a node contacted another node or surface. The constraint equation is such that the contacting node is forced to be on the contacted surface and allowed to slide, subject to the current friction conditions and the calculated tolerance zone. If a node slides from one segment to another during the iteration procedure, the retained nodes associated with the constraint are changed and a recalculation is automatically made. For tensile separation, a value of 10% of the maximum reaction force is used as the threshold limit.

Two separate published datasets (Table 1 and Table 2), both including muscle forces, were used to study the effects of load configuration on the predicted stability of cementless hip stems. The first dataset (Table 1) was obtained from the work of Duda [18,19] in which muscle and joint forces for two physiological activities, walking and stair climbing, were measured using telemetry. The second dataset (Table 2) was from the work of Fisher *et al*. [30], for the three distinct phases of a gait cycle–the heel-strike, the mid-stance and the toe-off. The directions of these muscle forces were derived from the geometric data extracted from the VHP dataset, and the magnitudes of the muscle forces and the hip joint contact forces were based on predictions by Brand and co-workers [31-32]. The loads reported by Fisher *et al*. [30] were significantly higher than the values measured by Duda and hence it was relevant to include both data sets in the analyses.

Table 1: Location of the muscles attachment used by Duda together with maximum loading configurations during walking and stair-climbing [18, 19]

Normal Walking Configuration	Force Components (N)		
	X	Y	Z
Joint contact force	-433.8	-263.8	1841.3
Abductor	465.9	34.5	-695.0
Tensor fascia lata, proximal part	57.8	93.2	-106.0
Tensor fascia lata, distal part	-4.0	-5.6	152.6
Vastus lateralis	-7.2	148.6	746.3
Stair Climbing Configuration	X	Y	Z
Joint contact force	-476.4	-486.8	1898.3
Abductor	563.1	231.4	-682.1
Ilio-tibial tract, proximal part	84.4	-24.1	-102.8
Ilio-tibial tract, distal part	-4.0	-6.4	135.0
Tensor fascia lata, proximal part	24.9	39.4	-23.3
Tensor fascia lata, distal part	-1.6	-2.4	52.2
Vastus lateralis	-17.7	180.0	1085.3
Vastus medialis	-70.7	318.1	2145.8

Table 2: Magnitudes of hip joint contact force and muscle forces for the
three phases of a gait cycle [30]

Force	Force Components (N)								
	1st phase (Heel strike)			2nd phase (Mid stance)			3rd phase (Toe-off)		
	X	Y	Z	X	Y	Z	X	Y	Z
Joint contact force	-857.3	-404.5	1722.5	-861.3	-250.8	2056.9	-613.7	-219.3	2868.7
Gluteus maximus	234.8	-37.6	-334.9	184.9	-85.2	-244	172.3	-105	-203.8
Gluteus medius	48.4	26.2	-93.7	42.2	-4	-81.7	63.7	-28.9	-113.3
	64.8	19.5	-85.1	56.5	-7.8	-72.2	85	-32.2	-97.4
	71.3	11.3	-81.2	62.1	-14.2	-66.4	92.3	-40.4	-87.1
Gluteus minimus	10.9	10	-21.4	21.5	7	-45.2	25.4	-0.7	-51.6
	13.5	4.1	-21.8	26.2	-5.1	-42.9	30.2	-14.4	-46.8
	19.5	-0.8	-17.2	37.6	-11.1	-31.9	43.2	-18.6	-33.2
Illiopsoas	0	0	0	-0.6	71.5	-60.8	3.6	160.6	-158.5
Piriformis	75.8	-26.0	-35.5	113.4	-61.6	-38	110.5	-70.1	-22.4
Adductor magnus	24.1	-6.9	-40.7	0	0	0	0	0	0
	20.3	-6.6	-42.7	0	0	0	0	0	0
	17.8	-6.1	-43.9	0	0	0	0	0	0
	15.8	-5.6	-44.8	0	0	0	0	0	0
Adductor minimus	17.1	4.3	-4.4	0	0	0	0	0	0
	15.9	3.2	-8.1	0	0	0	0	0	0
	14.1	2.5	-11.1	0	0	0	0	0	0
	12.3	1.9	-13.2	0	0	0	0	0	0

An in-house experimentally validated computer algorithm was used to measure micromotion at the interface and predict instability of the stem. This algorithm calculated the displacement of the stem relative to the endosteal surface of the bone by subtracting displacement values between corresponding nodes at the interface. From various threshold limits for bone ingrowth [15, 17, 33-34], a minimum micromotion value of 50μm was chosen. During the first iteration of the analysis, any areas with micromotion values lower than the threshold limit were adjusted by removing the elements to simulate interfacial bone loss (Figure 1). The iteration continues until either a stable-state interface micromotion was achieved or the implant failed. Implant failure occurred if interfacial shear strength

of 15MPa [35] was exceeded or the surface of the implant was encapsulated with the threshold micromotion limit representing fibrous tissue.
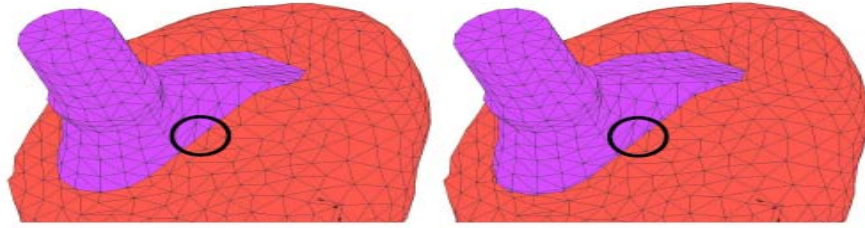

Figure 1: FE models showing no interference gaps (left) and with interfacial gaps with thickness of 500μm (right)

3.0   RESULTS

Figure 2 shows the cut-through model of the femoral bone used in this study, together with a picture taken from the CT dataset for comparison. The contour plot from FE using an in-house bone properties algorithm shows stiffness distribution within the femur, with stiff cortical bone of the long shaft showing higher stiffness than the proximal area surrounding the greater trochanter. The results show excellent agreement with the actual CT dataset used (lighter region corresponds to higher density and stiffness).
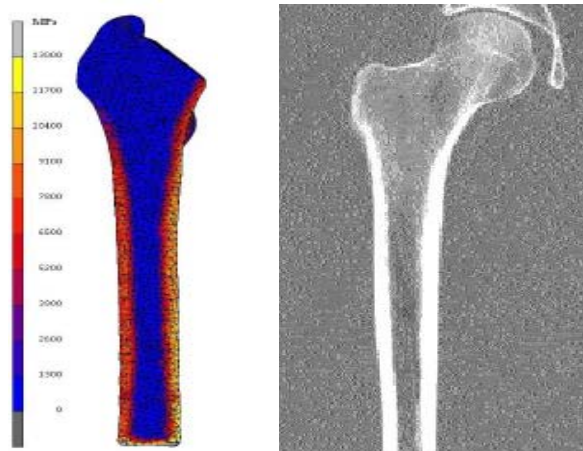

Figure 2: The contour plots of stiffness of femoral bone using the bone properties algorithm (left) and the corresponding image from the VHP CT dataset

Figure 3 shows that, in general, the distribution of micromotion is similar between loadcase 1 (with muscles) and loadcase 2 (without muscles), with the magnitude of micromotion in loadcase 1 being larger than in loadcase 2. With the

exception of the distal tip of the stem, distal regions are very stable compared to the proximal half.
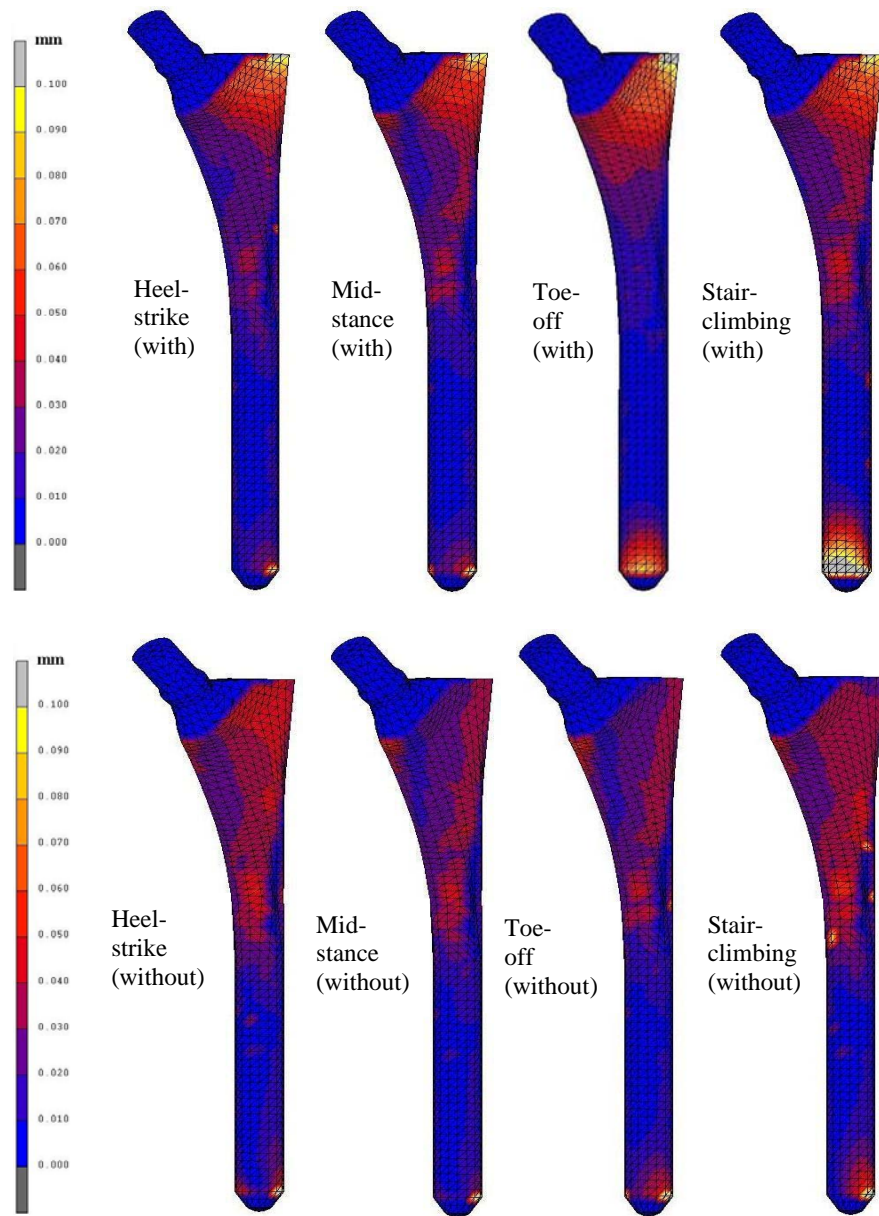
Figure 3: Contour plots of micromotion for the three phases of the gait cycle and for stairclimbing with muscle loads (top) and without muscle loads (bottom)

Table 3 shows that the areas with more than 50μm of micromotion are greater by up to 6 times in loadcase 1 than that in loadcase 2 at all phases of the gait cycle. For loadcase 1, the results for the heel-strike and the mid-stance are more or less similar, with a small increase in micromotion for the toe-off phase of the gait cycle. The difference in surface area exceeding the threshold limit is even greater-up to 20 times more in loadcase 1 than in loadcase 2 for Duda's loadcases.

Results using Duda's loadcases also show that stair-climbing activity is more critical than walking, because the surface area with micromotion beyond the chosen threshold limit of 50μm was doubled in stair-climbing. However, when compared to Fisher's toe-off phase of the gait cycle, the difference of the surface area was small.

Table 3: Surface area with more than 50μm of micromotion for the various loadcases

	Load Case		Area > 50μm (%)
With muscle loads	Walking	Heel strike	6
		Mid-stance	4
		Toe-off*	9
		Toe-off**	6
	Stair-climbing		11
Without muscle loads	Walking	Heel strike	1
		Mid-stance	1
		Toe-off*	2
		Toe-off**	0
	Stair-climbing		1

*Data from Fisher *et al.* [30]. **Data from Duda *et al.* [19]

4.0   DISCUSSION

The importance of including muscle loads in a study on hip arthroplasty is apparent. Apart from adequate description of the stress-strain distributions in a hip reconstruction [18-20] and accurately predicting bone resorption phenomena [21], muscle loads are also important in predicting loosening failure of hip arthroplasty. The FE results showed that ignoring muscle loads from FE analyses will under-estimate the interface micromotion, thus under-estimating the fibrous tissue formation and over-estimating the stability of the stems.

The results also showed that as the loading increased, the magnitude of micromotion also increased, thus increasing the chance of instability. This is in agreement with a study by Dickob and Martini [2] where patients who were overweight by 30% or more were found to be twice more likely to loosen their implants compared to patients with normal weight. Another follow-up study by Kim and Kim [36] reported that lower hip joint forces in patients with light body weight reduced the chance of implant loosening.

In Duda's loadcases, the results showed that stair-climbing was more critical because the surface area of potential fibrous tissue formation was almost twice as much as that in physiological walking. However, when compared with the toe-off

phase of the gait cycle from Fisher's loadcases, the results were almost similar in terms of magnitude, distribution of micromotion and surface area potential for bone ingrowth. This shows that the amount of micromotion, and therefore the stability, also depended on the loading vector, and not just by a specific type of activity. Toe-off phase of the gait cycle could be as critical to micromotion as stair-climbing. This has been confirmed by Pancanti *et al.* [37], who reported that for some patients, other tasks may be as critical as stair-climbing. Their micromotion study showed that the inter-subject variability had much more influence on the primary stability of cementless implants than the inter-task variability. Another paper by Kotzar *et al.* [38] also reported similar findings where in their telemeterized study, maximum torque during walking for some patients was found to be larger than during stair-climbing.

The FE results were also consistent with clinical findings. With a straight cylindrical stem design, distal regions normally have a higher potential for bone ingrowth due to strong cortical support [39-42]. Measurement of Bone Mineral Density (BMD) using Dual Energy X-ray Absorptiometry (DEXA) showed maximum bone loss occurred in the proximal femur. Bone atrophy usually took place around the greater trochanter area [17, 36, 43-45] and this is reflected in the FE analyses with micromotion in excess of the threshold limit of 50μm in the proximal region. Once the threshold limit is exceeded, fibrous tissue will take precedence over bone formation [46]. Optimum load transfer could not be achieved, and over time, the cancellous bone in the unloaded region will resorbed away.

Many have reported that the reason for such a phenomenon was the result of stiffness mis-match between the implant and the bone [36, 43-45]. Normal physiological loading could not be achieved with the Young's modulus of the implant exceeding five times the value of cortical bone. Problems with the rigidity of endosteal implants have led to the development of a more flexible stems, the so-called iso-elastic. The aim of iso-elasticity was to deform the implant and the bone as one unit, thus maintaining the structure of the bone under common loading conditions. In terms of maintaining bone stock, compliant stems have been shown to be better than stiff stems. An in-vivo study on canine models showed that reduced stem stiffness enhanced proximal load transfer thus reducing proximal bone loss [46]. In another study of 14 patients, where 6 patients had isoelastic implants, their overall BMD increased by a mean of 12.6%. For those with a relatively stiff titanium implant, the BMD decreased by a mean of 27% in the first year [47].

Though there seems to be an advantage of using isoelastic stems, several authors reported that the use of these stems caused high rate of loosening. Two of the now defunct hip prostheses, the RM prosthesis and the Morscher prosthesis, showed a high rate of aseptic loosening at follow-up period of nine years [48]. A later generation of isoelastic stems such as the prototype carbon fibre-reinforced composite also suffer a similar fate [49]. The authors reported macroscopic loosening and fibrous interface fixation for 92% of the implanted prostheses at 6 years post surgery. There seems to be a trade off between the rigid and flexible hip stems. Rigid implant minimizes micromotion at the interface, which is crucial for bone integration, but does not permit optimum load transfer to the bone. Flexible

implant on the other hand allows semi-physiological load transfer to the bone, but over time, causes unnecessary aseptic loosening due to excessive interface micromotion.

5.0   CONCLUSION

The results from this study showed the importance of including muscle forces in the prediction of hip stem stability.   Failure to include muscle forces will underestimate the interface micromotion, therefore overestimating the primary fixation of femoral stems.

REFERENCES

1. Clohisy, J.C. and Harris, W.H., 1999. The Harris-Galante uncemented femoral component in primary total hip replacement at 10 years, *The Journal of Arthroplasty*, 14(8), 915-917.
2. Dickob, M. and Martini, T., 1996. The cementless PM hip arthroplasty-Four-to-seven-year results, *Journal of Bone and Joint Surgery-British Volume*, 78B (2), 195-199.
3. Duparc, J. and Massin, P., 1992. Results of 203 total hip replacements using a smooth, cementless femoral component, *Journal of Bone and Joint Surgery-British Volume*, 74(2), 251-256.
4. Adam, F., Hammer, D.S., Pfautsch, S. and Westermann, K., 2002. Early failure of a press-fit carbon fiber hip prosthesis with a smooth surface, *Journal of Arthroplasty*, 17(2), 217-223.
5. Chen, C.H., Shih, C.H., Lin, C.C. and Cheng, C.K., 1998. Cementless roy-camille femoral component, *Archives of Orthopaedic and Trauma Surgery*, 118(1-2), 85-88.
6. Petersilge, W.J., Dlima, D.D., Walker, R.H. and Colwell, C.W., 1997. Prospective study of 100 consecutive Harris-Galante porous total hip arthroplasties - 4- to 8-year follow-up study, *Journal of Arthroplasty*, 12(2), 185-193.
7. Haddad, R.J., Cook, S.D. and Brinker, M.R., 1990. A comparison of 3 varieties of noncemented porous-coated hip-replacement, *Journal of Bone and Joint Surgery-British Volume*, 72(1), 2-8.
8. Jacobsson, S.A., Djerf, K., Gillquist, J., Hammerby, S. and Ivarsson, I., 1993. A prospective comparison of butel and PCA hip-arthroplasty, *Journal of Bone and Joint Surgery-British Volume*, 75(4), 624-629.
9. Karrholm, J., Anderberg, C., Snorrason, F., Thanner, J., Langeland, N., Malchau, H. and Herberts, P., 2002. Evaluation of a femoral stem with reduced stiffness-a randomized study with use of radiostereometry and bone

denistometry, *Journal of Bone and Joint Surgery-American Volume*, 84A(9), 1651-1658.

10. Bachus, K.N., Bloebaum, R.D. and Jones, R.E., 1999. Comparative micromotion of fully and proximally cemented femoral stems, *Clinical Orthopaedics and Related Research* 366, 248-257.

11. Berzins, A., Sumner, D.R., Andriacchi, T.P. and Galante, J.O., 1993. Stem curvature and load angle influence the initial relative bone-implant motion of cementless femoral stems, *Journal of Orthopaedic Research*, 11(5), 758-769.

12. Otani, T., Whiteside, L.A., White, S.E. and Mccarthy, D.S., 1993. Effects of femoral component material properties on cementless fixation in total hip arthroplasty, *Journal of Arthroplasty*, 8(1), 67-74.

13. Schneider, E., Eulenberger, J., Steiner, W., Wyder, D., Friedman, R.J. and Perren, S.M., 1989. Experimental-method for the invitro testing of the initial stability of cementless hip prostheses, *Journal of Biomechanics*, 22(6-7), 735-744.

14. Whiteside, L.A., Amador, D. and Russell, K., 1988. The effects of the collar on total hip femoral component subsidence, *Clinical Orthopaedics and Related Research* 231, 120-126.

15. Whiteside, L.A., White, S.E., Engh, C.A. and Head, W., 1993. Mechanical evaluation of cadaver retrieval specimens of cementless bone-ingrown total hip arthroplasty femoral components, *Journal of Arthroplasty*, 8(2), 147-155.

16. Burke, D.W., Oconnor, D.O., Zalenski, E.B., Jasty, M. and Harris, W.H., 1991. Micromotion of cemented and uncemented femoral components, *Journal of Bone and Joint Surgery-British Volume*, 73(1), 33-37.

17. Engh, C.A., Oconnor, D., Jasty, M., Mcgovern, T.F., Bobyn, J.D. and Harris, W.H., 1992. Quantification of implant micromotion, strain shielding and bone-resorption with porous-coated anatomic medullary locking femoral prostheses, *Clinical Orthopaedics and Related Research* 285, 13-29.

18. Duda, G., 1996. *Influence of muscle forces on the internal loads in the femur during gait,* Ph.D. thesis, Technische Universitat Hamburg.

19. Duda, G.N., Heller, M., Albinger, J., Schulz, O., Schneider, E. and Claes, L., 1998. Influence of muscle forces on femoral strain distribution, *Journal of Biomechanics*, 31(9), 841-846.

20. Kuiper, J.H. and Huiskes, R., 1996. Friction and stem stiffness affect dynamic interface in total hip replacement, *Journal of Orthopaedic Research*, 14(1), 36-43.

21. Kerner, J., Huiskes, R., van Lenthe, G.H., Weinans, H., van Rietbergen, B., Engh, C.A. and Amis, A.A., 1999. Correlation between pre-operative periprosthetic bone density and post-operative bone loss in THA can be explained by strain-adaptive remodelling, *Journal of Biomechanics*, 32(7), 695-703.

22. Ando, M., Imura, S., Omori, H., Okumura, Y., Bo, A. and Baba, H., 1999. Nonlinear three-dimensional finite element analysis of newly designed cementless total hip stems, *Artificial Organs*, 23(4), 339-346.

23. Biegler, F.B., Reuben, J.D., Harrigan, T.P., Hou, F. J. and Akin, J.E., 1995. Effect of porous coating and loading conditions on total hip femoral stem stability, *Journal of Arthroplasty*, 10(6), 839-847.

24. Keaveny, T.M. and Bartel, D.L., 1993. Effects of porous coating, with and without collar support, on early relative motion for a cementless hip-prosthesis, *Journal of Biomechanics*, 26(12), 1355-1368.

25. Rubin, P.J., Rakotomanana, R.L., Leyvraz, P.F., Zysset, P.K., Curnier, A. and Heegaard, J.H., 1993. Frictional interface micromotions and anisotropic stress distribution in a femoral total hip component, *Journal of Biomechanics*, 26(6), 725-739.

26. Viceconti, M., Monti, L., Muccini, R., Bernakiewicz, M. and Toni, A., 2001. Even a thin layer of soft tissue may compromise the primary stability of cementless hip stems, *Clinical Biomechanics*, 16(9), 765-775.

27. Viceconti, M., Muccini, R., Bernakiewicz, M., Baleani, M. and Cristofolini, L., 2000. Large-sliding contact elements accurately predict levels of bone-implant micromotion relevant to osseointegration, *Journal of Biomechanics*, 33(12), 1611-1618.

28. Kendrick, J.B., Noble, P.C. and Tullos, H.S., 1995. Distal stem design and the torsional stability of cementless femoral stems, *Journal of Arthroplasty*, 10(4), 463-469.

29. Carter, D. and Hayes, W., 1997. The compressive behaviour of bone as a two-phase porous structure, *Journal of Bone and Joint Surgery*, 59(7), 954-962.

30. Fisher, I.A., 2000. *A mathematical investigation of the influence of skeletal geometry on the mechanics of a prosthetic human hip joint*, PhD Thesis, Imperial College London.

31. Brand, R., Pederson, D. and Friederich, J., 1986. The sensitivity of muscle force predictions to changes in physiologic cross-sectional area, *Journal of Biomechanics*, 19(8), 589-596.

32. Brand, R., Pederson, D., Davy, D., Kotzar, G., Heiple, K. and Goldberg, V., 1994. Comparison of hip force calculations and measurements in the same patient, *Journal of Arthroplasty*, 9(1), 45-51.

33. Maloney, W.J., Jasty, M., Burke, D.W., Oconnor, D.O., Zalenski, E.B., Bragdon, C. and Harris, W.H., 1989. Biomechanical and histologic investigation of cemented total hip arthroplasties-a study of autopsy-retrieved femurs after invivo cycling, *Clinical Orthopaedics and Related Research* 249, 129-140.

34. Szmukler-Moncler, S., Salama, H., Reingewirtz, Y. and Dubruille, J.H., 1998. Timing of loading and effect of micromotion on bone-dental implant interface: Review of experimental literature, *Journal of Biomedical Materials Research*, 43(2), 192-203.

35. Dhert, W.J.A. and Jansen, J.A., 2000. The validity of a single pushout test, in *Mechanical testing of bone and the bone-implant interface*, 1st edn, Y.H. An and R.A. Draughn, eds., CRC Press.

36. Kim, Y.H. and Kim, V.E.M., 1994. Cementless porous-coated anatomic medullary locking total hip prostheses, *The Journal of Arthroplasty*, 9(3), 243-252.

37. Pancanti, A., Bernakiewicz, M. and Viceconti, M., 2003. The primary stability of a cementless stem varies between subjects as much as between activities, *Journal of Biomechanics*, 36(6), 777-785.

38. Kotzar, G.M., Davy, D.T., Berilla, J. and Goldberg, V.M., 1995. Torsional loads in the early postoperative period following total hip replacement, *Journal of Orthopaedic Research*, 13(6), 945-955.

39. Ang, K.C., De, S.D., Goh, J.C.H., Low, S.L. and Bose, K., 1997. Periprosthetic bone remodelling after cementless total hip replacement-a prospective comparison of two different implant designs, *Journal of Bone and Joint Surgery-British Volume*, 79B(4), 675-679.

40. Badhe, N.P., Quinnell, R.C. and Howard, P.W., 2002. The uncemented Bi-Contact total hip arthroplasty, *The Journal of Arthroplasty*, 17, 7, 896-901.

41. Callaghan, J.J., Fulghum, C.S., Glisson, R.R. and Stranne, S.K., 1992. The effect of femoral stem geometry on interface motion in uncemented porous-coated total hip prostheses- comparison of straight-stem and curved-stem designs, *Journal of Bone and Joint Surgery-American Volume*, 74A(6), 839-848.

42. Whiteside, L.A., 1989. The effect of stem fit on bone hypertrophy and pain relief in cementless total hip-arthroplasty, *Clinical Orthopaedics and Related Research* 247, 138-147.

43. Chess, D.G., Grainger, R.W., Phillips, T., Zarzour, Z.D. and Pard, B.R., 1996. The cementless anatomic medullary locking femoral component: An independent clinical and radiographic assessment, *Canadian Journal of Surgery*, 39(5), 389-392.

44. Engh, C.A., Hooten, J.P., Zettlschaffer, K.F., Ghaffarpour, M., Mcgovern, T.F., Macalino, G.E. and Zicat, B.A., 1994. Porous-coated total hip-replacement, *Clinical Orthopaedics and Related Research* 298, 89-96.

45. Johnston, D.W.C., Davies, D.M., Beaupre, L.A. and Lavoie, G., 2001. Standard anatomical medullary locking (AML) versus tricalcium phosphate-coated AML femoral prostheses, *Canadian Journal of Surgery*, 44(6), 421-427.

46. Pilliar, R.M., Lee, J.M. and Maniatopoulos, C., 1986. Observations on the effect of movement on bone ingrowth into porous-surfaced implants, *Clinical Orthopaedics and Related Research* 208, 108-113.

47. Sumner, D.R., Turner, T.M., Urban, R.M. and Galante, J.O., 1991. Bone ingrowth into porous coatings attached to prosthesis of differing stiffness, in *The Bone Biomaterial Interface*, University of Toronto Press.

48. Morscher, E.W. and Dick, W., 1983. Cementless fixation of isoelastic hip endoprostheses manufactured from plastic materials, *Clinical Orthopedics and Related Research*, 176, 77-87.

49. Adam, F., Hammer, D.S., Pfautsch, S. and Westerman, K., 2002. Early failure of a press-fit carbon fiber hip prosthesis with a smooth surface, *Journal of Arthroplasty*, 17(2), 217-223.